

Search for a 17 keV neutrino in the internal bremsstrahlung spectrum of  $^{125}\text{I}$ 

M. M. Hindi, R. L. Kozub, and S. J. Robinson

*Physics Department, Tennessee Technological University, Cookeville, Tennessee 38505*

(Received 27 January 1994)

We have searched for evidence of the emission of a 17 keV neutrino in the internal bremsstrahlung (IB) spectrum accompanying the electron capture decay of  $^{125}\text{I}$ . The IB spectrum, recorded in a planar Ge detector, has  $1.2 \times 10^6$  counts per keV at 17 keV below the  $2p$  end point. We set an upper limit of 0.4% for the admixture of a 17 keV neutrino, at the 90% confidence level, and exclude a 0.8% admixture at the 99.6% confidence level. The  $Q_{\text{EC}}$  value is found to be  $185.77 \pm 0.06$  keV. We also find that the recent calculations of Surić *et al.*, which employ relativistic self-consistent-field atomic wave functions, reproduce the shape and relative intensity of IB partial spectra within a few percent.

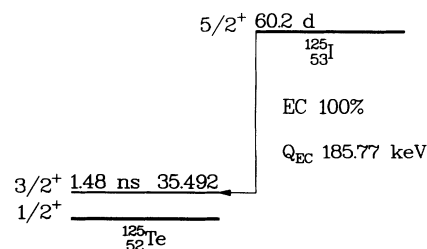
PACS number(s): 23.40.-s, 14.60.Pq, 27.60.+j

## I. INTRODUCTION

There have been claims of observation of a massive ( $\approx 17$  keV) neutrino in the beta spectra of  $^3\text{H}$  [1,2],  $^{14}\text{C}$  [3],  $^{35}\text{S}$  [4,5],  $^{63}\text{Ni}$  [6], and in the internal bremsstrahlung (IB) spectrum of  $^{71}\text{Ge}$  [7]. These claims are contradicted by experiments on  $^3\text{H}$  [8,9],  $^{35}\text{S}$  [10-12],  $^{63}\text{Ni}$  [13,14],  $^{55}\text{Fe}$  [15],  $^{71}\text{Ge}$  [16],  $^{125}\text{I}$  [17], and  $^{177}\text{Lu}$  [18]. If neutrino mixing does occur, then it should be a universal phenomenon and should occur in electron capture decay, as well as in beta decay. We have conducted an experiment to search for the admixture of a 17 keV neutrino in the IB spectrum of  $^{125}\text{I}$ . A search for neutrino mixing in the IB spectrum of  $^{125}\text{I}$  has been conducted before by Borge *et al.* [17], but that experiment was designed to test the initial claim [1] of a mixing fraction of about 2-4% and it does not reject the later claims of  $\approx 1\%$  mixing fraction with a high degree of statistical confidence. Although some of the most recent negative experiments [15,14,11] reject the 17 keV neutrino hypothesis with a high degree of confidence, and although a consensus that the 17 keV neutrino does not exist is emerging, we feel it is worthwhile to present our data (which were collected in 1992 [19]) for the following reasons. Since all of the positive claims were obtained with solid state detectors, while many of the negative results were obtained with magnetic spectrometers, there have been suggestions [20] that the kinks in the observed spectra are possibly due to solid state effects. Our negative result, which was obtained using a solid state detector, suggests that such is probably not the case. The signature in  $^{125}\text{I}$  for a 17 keV neutrino is dominated by *two* kinks, one 17 keV below the  $2p$  IB end point ( $E \sim 128$  keV), and one 17 keV below the  $3p$  IB end point ( $E \sim 132$  keV). This signature is qualitatively different from that appearing in the studies reported thus far, namely a spectrum dominated by *one* kink. In addition to providing an independent test of the 17 keV neutrino hypothesis, our high statistics data also provide a stringent test of the recent IB calculations of Surić *et al.* [21]. These calculations are fully relativistic and take screening into account by employing atomic wave func-

tions obtained using a relativistic self-consistent field in an independent particle approximation. To our knowledge, only the data of Wietfeldt *et al.* [15] on  $^{55}\text{Fe}$  have higher statistics (in IB studies) than ours, but they did not use theoretical IB spectral shapes in their analysis. The data of Borge *et al.* [17] on  $^{125}\text{I}$  have considerably lower statistics than ours, and have been analyzed using a nonrelativistic calculation. Finally, the  $Q_{\text{EC}}$  value of  $186.1 \pm 0.3$  keV obtained by Borge *et al.* [17] is in disagreement with a more recent, albeit less accurate, value of  $179.3 \pm 2.0$  keV obtained by Flower *et al.* [22]. Our data give a more accurate  $Q_{\text{EC}}$  value for  $^{125}\text{I}$  ( $185.77 \pm 0.06$  keV), which is in much better agreement with Borge *et al.*'s value.

The decay scheme of  $^{125}\text{I}$  is shown in Fig. 1. The decay to the first excited state of  $^{125}\text{Te}$  at 35.5 keV is an allowed transition, while the decay to the ground state is a second-forbidden nonunique transition. From the systematics of second-forbidden nonunique transitions [23] one obtains a  $\log ft$  value  $> 11$ , which corresponds to a branch of  $< 4.4 \times 10^{-4}\%$  for the decay to the ground state in  $^{125}\text{Te}$ . Thus, for our purposes, IB associated with decay to the ground state, if present at all, can be ignored. Because of this exclusive decay to the excited state, whose decay radiation is easily attenuated relative to the higher energy IB radiation, and the relatively low end-point energy of 150.3 keV,  $^{125}\text{I}$  presents a favorable case for the study of IB spectra and for the search for a 17 keV neutrino.

FIG. 1. Decay scheme of  $^{125}\text{I}$ . The level energy is in keV.

## II. EXPERIMENTAL PROCEDURE

A 200 mCi  $^{125}\text{I}$  source was purchased from Amersham Corporation. The  $^{125}\text{I}$  is incorporated in a resin bead 1 mm in diameter which is sealed in an aluminum alloy capsule and mounted in a stainless steel holder with a 5  $\mu\text{m}$  titanium window. Gamma rays emitted by the source were detected in an intrinsic planar Ge detector with a 16 mm diameter, 10 mm depth, and a 0.128-mm-thick Be window. Four copper sheets, each 0.5 mm thick, and backed by several Al foils with a total thickness of 0.5  $\text{mg}/\text{cm}^2$ , were placed between the source and the detector. In addition to reducing the count rate of the Te x rays and the 35.5-keV  $\gamma$  rays in the detector, the copper served to reduce the summing probability of IB with x rays to negligible levels. (Since  $^{125}\text{I}$  decays 100% of the time to the first excited state of  $^{125}\text{Te}$ , the IB is always accompanied by internal conversion x rays or 35.5-keV  $\gamma$  rays from the decay of that level; thus, true summing of x rays or 35.5-keV  $\gamma$  rays with the IB is possible, leading to a distortion of the measured IB spectrum.) The transmission of probability the 35.5-keV  $\gamma$  rays through the copper sheets was measured to be  $6 \times 10^{-6}$  and that of the Te x rays to be  $2 \times 10^{-8}$ . These transmission probabilities then result in a total summing probability of less than  $1 \times 10^{-7}$ , which is negligible. In the above counting geometry the distance between the source and the Ge crystal was  $\approx 8$  mm. The detector and source were surrounded by a graded shield made of 0.1-cm-thick Al plates, 0.95-cm-thick Cu plates, and 10.2-cm-thick lead bricks.

The signal from the preamplifier was fed into two amplifiers (ORTEC models 570 and 572) with 1- $\mu\text{s}$  shaping times, but with different gains. One of the amplifiers (ORTEC 572) was equipped with pileup rejection circuitry. The amplifier signals were digitized in two channels of a 13-bit (8192 channels) CAMAC analog-to-digital converter (ADC, ORTEC model AD413), with dispersions of 33 eV and 39 eV per channel. This duplication of signals served as a check that any observed distortion in the spectrum was not an artifact of the amplifiers or the ADC.

Four separate spectra were collected (pileup-accepted and pileup-rejected spectra for each of the two amplifiers) using a VAX 11/730 computer. The spectra were saved to disk every 12 h. Counting with the  $^{125}\text{I}$  source in place lasted for 71 days. The count rate at the beginning of the counting period was  $650 \text{ s}^{-1}$  and the final rate was  $290 \text{ s}^{-1}$ . The gain stability of the system was monitored by collecting spectra of  $^{109}\text{Cd}$ ,  $^{57}\text{Co}$ , and  $^{133}\text{Ba}$  every 3–4 days, with the  $^{125}\text{I}$  source in place. Room background spectra were collected for a period of 10 days before collecting the  $^{125}\text{I}$  spectra and for a period of 7 days afterwards, for a total of 17 days.

To determine the response function of the detector to photons in the energy region of interest, we collected spectra of calibrated point sources of  $^{109}\text{Cd}$  and  $^{57}\text{Co}$ ; for energy calibrations  $^{133}\text{Ba}$  was used in addition to these sources. The energy resolution of the system at 122 keV was 560 eV.

The relative efficiency was determined using a  $^{182}\text{Ta}$

source. To avoid summing, the  $^{182}\text{Ta}$  spectra were taken with the source at distances of 6 cm and 8 cm from the normal position of the  $^{125}\text{I}$  source (0.8 cm from the detector). The possible variation in the relative efficiency as a function of distance from the detector was examined by looking at the ratio of yields of lines from  $^{109}\text{Cd}$  and  $^{57}\text{Co}$  as a function of distance. The change in the ratio of the 88-keV-to-136-keV lines, as the source was moved from 0.8 cm to 8 cm, was found to be  $< 3\%$ , and the change in the ratio of the 122-keV-to-136-keV lines was found to be  $< 1\%$ .

The dynamic range of the preamp-amp combination on the planar detector allowed a maximum photon energy of  $\approx 320$  keV to be observed. To check for contaminant lines at higher energies (up to 2.7 MeV) radiation from the source was counted in a 91  $\text{cm}^3$  coaxial Ge detector for 10.7 days and the background for 6.5 days. Lines were observed from the decay of  $^{126}\text{I}$ , which Amersham had indicated was present in the source at a level  $< 5 \times 10^{-5}$ . We confirmed that the lines are due to  $^{126}\text{I}$  by following the decay curve of their activity and finding a half-life of  $12.2 \pm 2.1$  days, which agrees with the  $^{126}\text{I}$  half-life of 13.0 days. A long-lived line at 662 keV, which we ascribe to  $^{137}\text{Cs}$ , was also observed. Since the source was made in a reactor by neutron capture on enriched  $^{124}\text{Xe}$  gas [ $^{124}\text{Xe} + n \rightarrow ^{125}\text{Xe}(17 \text{ h}) \xrightarrow{\text{EC}} ^{125}\text{I}$ ], the  $^{137}\text{Cs}$  could have been produced by neutron capture on residual amounts of  $^{136}\text{Xe}$  in the gas [ $^{136}\text{Xe} + n \rightarrow ^{137}\text{Xe}(3.8 \text{ min}) \xrightarrow{\beta^-} ^{137}\text{Cs}$ ]. A search was conducted for other contaminants, especially those that can be produced from neutron interactions with the other stable isotopes of Xe; no evidence for any other contaminant lines was found.

The  $^{125}\text{I}$  IB spectra presented here were collected beginning approximately 3 months after arrival of the source, at which point the  $^{126}\text{I}$  had decayed to a negligible level. To determine the contribution of the  $^{137}\text{Cs}$  contaminant, spectra of a calibrated  $^{137}\text{Cs}$  point source were measured in each of the planar and coaxial Ge detectors. The procedures for subtracting the  $^{137}\text{Cs}$  and background spectra from the  $^{125}\text{I}$  source spectrum are described in the next section.

## III. DATA REDUCTION

Before consolidating the 12-h spectra into a single spectrum, the stability of both the gain and the energy resolution was checked by measuring the centroids and widths of peaks in the calibration spectra as well as the 35.5-keV  $\gamma$ -ray peak in the  $^{125}\text{I}$  spectra. The standard deviation of the centroids of peaks was 15 eV and that of the widths was 2 eV. These deviations are small compared to the energy resolution of the detector (560 eV at 122 keV). Hence, all the  $^{125}\text{I}$  spectra and background spectra were summed together, without applying any shifts.

Figure 2 shows the total raw  $^{125}\text{I}$  spectrum (with electronic pileup rejection) for ADC 1, compressed 8 channels to a bin (0.311 keV per bin). The total live counting time is 61 days. Also shown are the background,  $^{137}\text{Cs}$ , and residual pileup spectra. These spectra are normal-

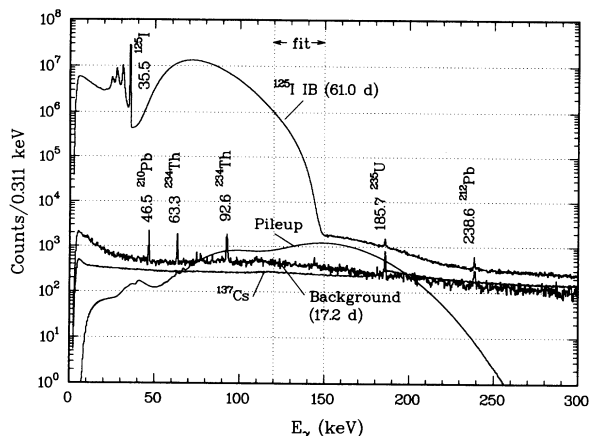


FIG. 2. Spectra of the  $^{125}\text{I}$  source and of the scaled background,  $^{137}\text{Cs}$  contaminant, and pileup.  $\gamma$ -ray energies are given in keV.

ized properly (in a manner to be described below), so that their relative contribution can be deduced from the figure. The region of the IB spectrum which was used in searching for a 17 keV neutrino was from 120 to 150.5 keV. The raw spectrum has  $1.2 \times 10^6$  counts per keV at 17 keV below the  $2p$  end point (128.6 keV). At that point the background contribution is 0.11%, the  $^{137}\text{Cs}$  0.07%, and the pileup 0.25%.

The background spectrum represents a total counting period of 17.2 days and has been multiplied by a factor of 3.54, the ratio of live counting times for the  $^{125}\text{I}$  and background spectra. This ratio is in agreement with the ratio of the full energy peak counts of the  $^{235}\text{U}$  line at 185.7 keV and the  $^{212}\text{Pb}$  line at 238.6 keV in the two spectra ( $3.31 \pm 0.28$ ). The effect of a systematic change of  $\pm 6\%$  in the background normalization factor has been investigated and is described later. The  $^{137}\text{Cs}$  spectrum from the calibration source was normalized to the raw  $^{125}\text{I}$  spectrum in the energy range 290–311 keV, after background subtraction. In this energy region the pileup contribution is negligible. The resulting normalization factor (0.077) agrees well with the normalization factor of  $0.078 \pm 0.003$ , obtained from the ratio of the yields of the 662-keV line, measured in the 91-cm<sup>3</sup> coaxial Ge detector.

The shape of the residual pileup spectrum was computed with the assumption that it is due to events which occur sufficiently close in time to escape the pileup rejection circuitry of the amplifier (measured resolving time of 300 ns). In that case the two events should produce a pulse with height equal to approximately the sum of the heights of the pulses due to the individual events. The resulting pileup spectrum can then be obtained by convoluting the raw  $^{125}\text{I}$  spectrum with itself, subtracting the result from the raw  $^{125}\text{I}$  spectrum to obtain a first-order pileup-corrected spectrum, and then repeating the process using the new  $^{125}\text{I}$  spectrum, until the process has converged. The pileup spectrum was normalized by fitting it to the  $^{125}\text{I}$  spectrum in the region above the end point, after background and  $^{137}\text{Cs}$  subtraction. Figure 3 shows the resulting portion of the  $^{125}\text{I}$  spectrum above

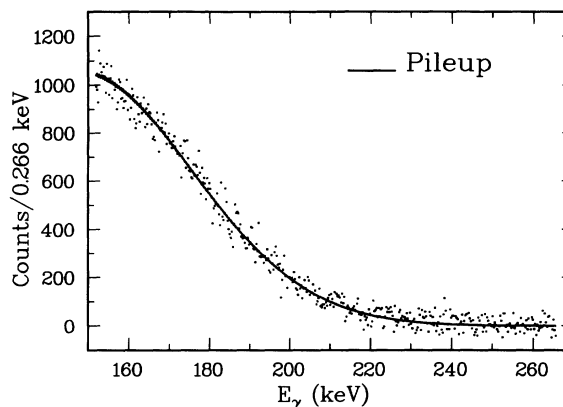


FIG. 3. The data points show the portion of the spectrum above the IB end point, after background and  $^{137}\text{Cs}$  subtraction; the solid line shows the pileup spectrum, obtained as described in the text.

the end point, together with the computed pileup spectrum. The fit with one parameter (normalization factor) has a  $\chi^2$  of 503 for 425 degrees of freedom (reduced  $\chi^2$  of 1.18). The resulting statistical error in the normalization factor is 0.5%; the effect of a change of  $\pm 0.5\%$  in the pileup normalization factor has been investigated and is described below.

After subtracting the room background, the contribution of the  $^{137}\text{Cs}$  contaminant, and the residual pileup, the spectra were compressed to 8 channels per bin [0.311 keV per bin for the spectrum collected via the first amplifier-ADC combination (ADC/AMP 1), and 0.266 keV per bin for the spectrum collected with the second amplifier-ADC combination (ADC/AMP 2)].

The energy scale of the spectrum was determined using the  $^{109}\text{Cd}$  88.0341-keV line [24], the  $^{57}\text{Co}$  lines at 122.0614 and 136.4743 keV [24], and the  $^{133}\text{Ba}$  line at 160.613 keV [25]. The residuals of the fits using a linear energy calibration were less than 4 eV.

The response function of the detector to gamma rays was measured using the  $^{109}\text{Cd}$  and  $^{57}\text{Co}$  lines. Figure 4 shows the 122-keV line of  $^{57}\text{Co}$  and the response shape which was used. The response shape was parametrized as the sum of a Gaussian peak, an exponential tail on the low energy side (which arises mainly from forward scattering in the Cu absorber), Ge  $K\alpha$  and  $K\beta$  x-ray escape peaks, and a flat tail. Both the exponential tail and the flat tail were convoluted with a Gaussian that had the same width as the main Gaussian peak, so these components did not drop sharply to zero at the peak centroid, but smoothly, with a width reflective of the detector resolution. The shape parameters were interpolated as a function of photopeak energy from the shape parameters obtained for the  $^{109}\text{Cd}$  and  $^{57}\text{Co}$  lines. It should be noted here that the low energy part of the response function includes a pronounced backscatter peak, which cannot be adequately reproduced with a flat tail. In the present application, however, the energy region being fitted (when searching for a 17 keV neutrino) is 120–150 keV. For such an energy range the backscattered peak is at  $\leq 94$  keV, and hence the fitting region always falls on the flat (or

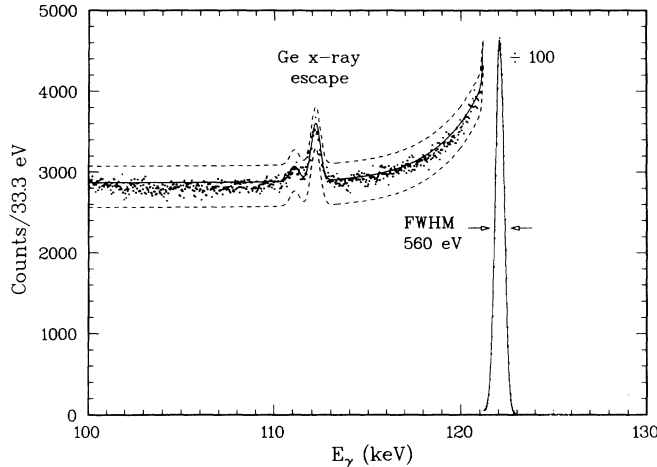


FIG. 4. The data points show the response of the planar HPGe detector to the  $^{57}\text{Co}$  122-keV line; the solid line shows the parametrized line shape which modeled the response. The dashed lines show the limits which were used in the systematics tests.

exponential) part of the tail of the higher energy gamma rays.

The relative efficiency of the planar Ge detector, as a function of photopeak energy, was obtained from the  $^{182}\text{Ta}$  spectra. The intensities of the  $^{182}\text{Ta}$  lines were obtained from the recent measurements of Kempisty and Pochwalski [26]. The measured efficiencies were fitted as a function of energy with the functional form

$$\epsilon(E) = (a_1 E - 1) (a_2 e^{-a_3 E} + a_4), \quad (1)$$

where the  $a_i$ 's are the fitting parameters. Figure 5 shows the measured efficiencies for the spectrum collected at 8

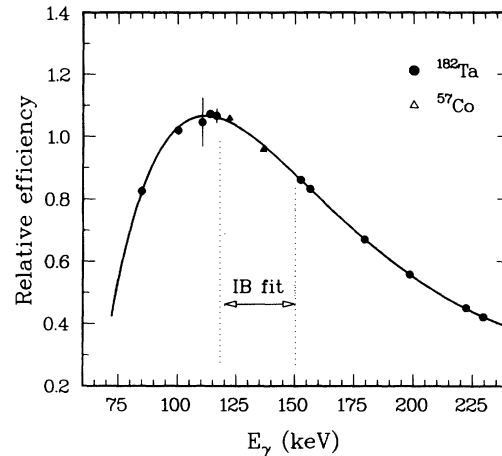


FIG. 5. Relative efficiency of the detector. The data points (solid circles) are from  $^{182}\text{Ta}$  lines with the source at 8 cm from the detector. The solid line is the fit. The open triangles are from the  $^{57}\text{Co}$  lines with the source at 0.8 cm.

cm, and the resultant fit. Also shown, for comparison, are the relative efficiencies of the  $^{57}\text{Co}$  lines, measured at the position of the  $^{125}\text{I}$  source.

#### IV. DATA ANALYSIS AND RESULTS

After subtracting the contributions of pileup, room background, and the  $^{137}\text{Cs}$  contaminant, the region from 120 to 150.5 keV was fit with a theoretical shape that was convoluted with the measured response function and integrated over the width of a bin. The theoretical IB spectral shape is given by

$$\frac{dW(E, m)}{dE} = \sum_{n,j} \eta_{nj} |M_{nj}(E)|^2 E (Q_0 - B_{nj} - E) [(Q_0 - B_{nj} - E)^2 - m^2]^{1/2}, \quad (2)$$

where  $E$  is the IB photon energy,  $m$  is the mass of the neutrino,  $M_{nj}(E)$  is the energy-dependent IB matrix element for capture from subshell  $j$  in the major shell  $n$ ,  $\eta_{nj}$  is the number of electrons in the orbital  $nj$ ,  $Q_0$  is the energy of the transition, and  $B_{nj}$  are the atomic binding energies in the daughter atom (tellurium). The summation runs over all the filled orbitals in the parent (iodine) for which a transition is energetically allowed, i.e., for which  $E < Q_0 - B_{nj} - m$ . The atomic binding ener-

gies were obtained from the tables of Larkins [27]. The IB electron capture (IBEC) matrix elements were calculated using the code developed by Surić, Horvat, and Pisk [21]. This code calculates IBEC matrix elements in an independent-particle approximation, with atomic wave functions obtained from a relativistic self-consistent-field potential.

The fitting function which was used is

$$\frac{dN(E)}{dE} = A [1 + a_1(E - 151 \text{ keV})] \int_E^{E+\Delta E} dE'' \int_0^\infty \left[ (1-c) \frac{dW(E', 0)}{dE'} + c \frac{dW(E', m)}{dE'} \right] R(E'', E') dE'. \quad (3)$$

It contains an incoherent sum of IBEC spectra associated with the emission of two neutrinos, one with zero mass and emission probability  $1 - c$  and the other with mass  $m$  and emission probability  $c$ . The theoretical spectral shape is convoluted with the response function  $R(E'', E')$

of the detector, and the result integrated over the binning width  $\Delta E$  of the data (311 eV for ADC/AMP 1, 266 eV for ADC/AMP 2) [28]. To absorb possible deviations of the theoretical shape from the true spectral shape, and to account for any residual smooth variations in the

efficiency, response function, and pileup subtraction, the spectrum is multiplied by a linear shape factor of the form  $P(E) = 1 + a_1(E - 151 \text{ keV})$ , where the parameter  $a_1$  is allowed to vary freely.

Since the ability of the current IB theory to reproduce the absolute magnitudes of the IB spectra from different shells has not, to our knowledge, been tested to the level necessary for the current study, we allow in the fitting procedure the possibility of including an independent scaling parameter for each of the  $n_j$  IB components. [That is, in Eq. (2) we replace  $|M_{nj}(E)|^2$  by  $r_{nj}|M_{nj}(E)|^2$ .] To reduce the number of free parameters, we have restricted the fitting region to 120–150.5 keV; therefore, the  $1s$  component, which has an end point of 118.4 keV, does not enter the fit. The difference in end points between the different subshells  $j$  for a given  $n$  is not sufficient to enable an independent normalization of each in the fit; i.e., if one allowed the normalization of both the  $2s$  and  $2p$  components (or the  $3p$  and  $3s$  components) to vary simultaneously, one would get large and highly correlated errors on the normalizations of the  $s$  and  $p$  components. Also, since the contribution of IB from shells with  $n > 3$  is small over most of the fitting region and contributes independently only over the last 0.8 keV of the spectrum, no attempt was made to scale the contribution of shells with  $n > 3$  independently. Therefore, in the final fits presented here, only the scaling parameter of the  $n = 3$  shell was allowed to vary freely. Thus, in the fitting procedure, four parameters were allowed to vary freely: an overall normalization parameter  $A$ , the scaling parameter  $r$  ( $\equiv r_{3j}$ ) of the  $n = 3$  IB spectrum, the end-point energy  $Q_0$ , and the linear shape parameter  $a_1$ .

To search for massive neutrinos a least-squares fit of the data to the shape described above was conducted. For a given value of the pair  $(m, c)$  the  $\chi^2$  value was minimized by allowing the parameters  $A$ ,  $r$ ,  $Q_0$ , and  $a_1$  to vary freely. This procedure was conducted for the data collected through both ADC/AMP 1 (98 data points) and ADC/AMP 2 (114 data points). Figure 6 shows the resulting  $\chi^2$  contours. For ADC/AMP 1 the  $\chi^2$  value for a single massless neutrino is 102.8. (The probability of obtaining a smaller  $\chi^2$  for 94 degrees of freedom is 75.0%.) The absolute minimum of  $\chi^2$  in the region searched is 100.2 [at  $(m = 24.5 \text{ keV}, c = 0.6\%)$ ]. According to statistical theory, if the null hypothesis holds, i.e., if the data are well represented by a fit with one massless neutrino, then the difference in the  $\chi^2$  value between a fit with a single massless neutrino and a fit with two additional parameters ( $m$  and  $c$ ) should itself be distributed like a  $\chi^2$  distribution with two degrees of freedom. Therefore, if the two additional parameters are superfluous, the expected improvement in the  $\chi^2$  is about 2 units. The local minimum at  $(m = 24.5 \text{ keV}, c = 0.6\%)$ , which is lower by 2.6 units than the  $\chi^2$  for a single massless neutrino, corresponds to a confidence level of 73%, and hence is not statistically very significant. The  $\chi^2$  for a 17 keV neutrino with a mixing probability of 0.8%, the lowest central positive value reported in the literature [5], is 114.6, i.e., 14.4 units higher than the minimum, and hence can be excluded at the 99.93% confidence level. The upper limit

on the mixing fraction of a 17 keV neutrino is 0.4%, at the 90% confidence level.

To test for the possible dependence of the above results on amplifier or ADC nonlinearities, the data routed through AMP/ADC 2 (0.266 keV per bin, 114 data points) were also analyzed in the same manner. The corresponding results are for a massless neutrino  $\chi^2 = 110.6$  (the probability of obtaining a smaller  $\chi^2$  for 110 degrees of freedom is 53.5%); absolute local minimum of  $\chi^2 = 109.5$  at  $(m = 25.0 \text{ keV}, c = 0.6\%)$ , which is 1.1 units lower than that with a massless neutrino and corresponds to a confidence level of 42%; the  $\chi^2$  for a 17 keV neutrino with a mixing probability of 0.8% is 120.5, and hence is excluded at the 99.6% confidence level. The limit on a 17 keV neutrino is 0.4%, at the 90% confidence level.

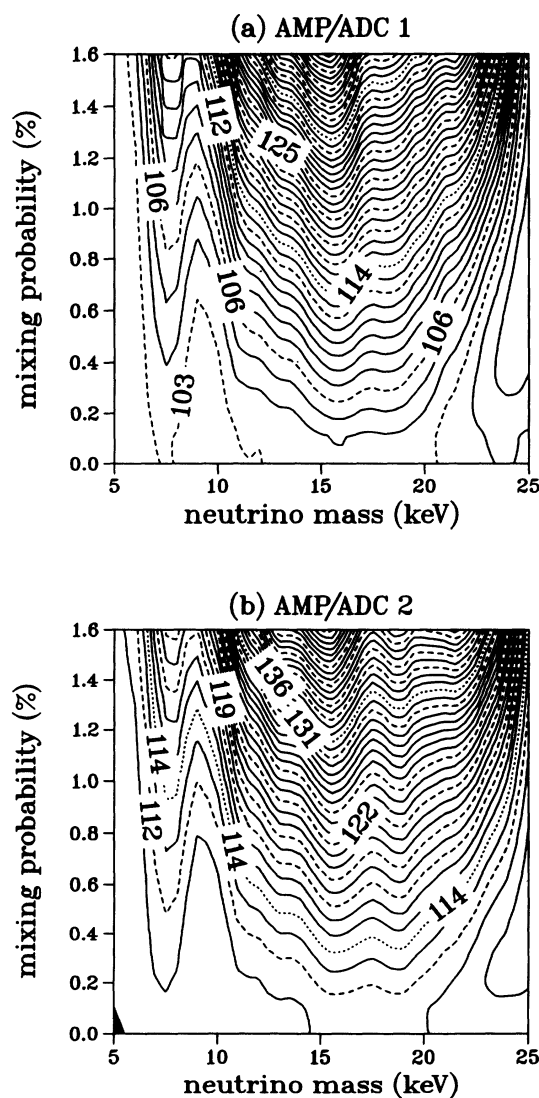


FIG. 6. Contour lines of  $\chi^2$  as a function of neutrino mass and mixing probability. (a) Data collected through ADC/AMP 1 (98 data points). The  $\chi^2$  for zero mixing is 102.8; the minimum is 100.2 at  $(m = 24.5 \text{ keV}, c = 0.6\%)$ . (b) Data collected through ADC/AMP 2 (114 data points). The  $\chi^2$  for zero mixing is 110.6; the minimum is 109.5 at  $(m = 25.0 \text{ keV}, c = 0.6\%)$ .

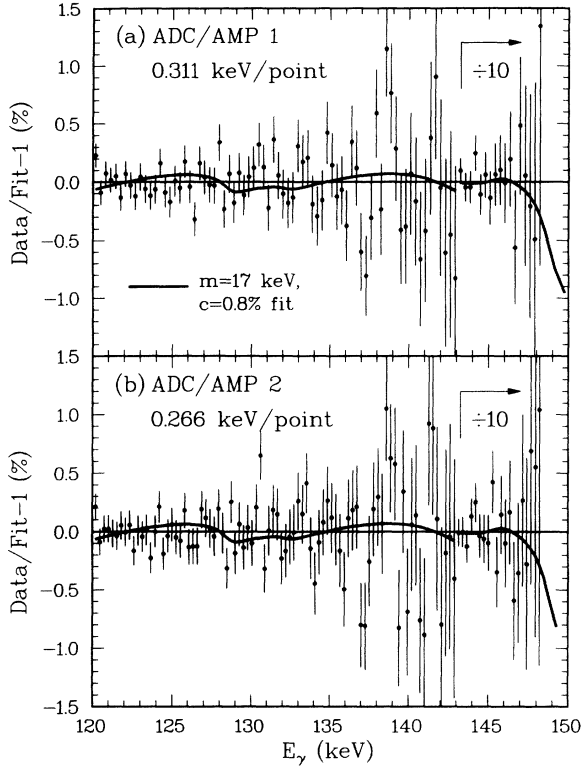


FIG. 7. (a) Ratio of experimental data to the theoretical fit with a single massless neutrino. The solid curve is the ratio of the theoretical fit obtained with  $m = 17$  keV,  $\sin^2 \theta = 0.8\%$  to the theoretical fit with  $m = 0$ . The data are those obtained through ADC/AMP 2. (b) Same as (a) for data obtained through ADC/AMP 1.

Figures 7(a) and 7(b) show, respectively, for ADC/AMP 1 and ADC/AMP 2, the ratio of the data to the fit for massless neutrinos; the solid curves show the ratio of the fit for a 17 keV neutrino with a mixing fraction of 0.8% to that obtained with  $m = 0$ . The fit parameters are listed in Table I. The systematic errors appearing in the table are discussed below. The agreement in the values of the parameters extracted from the two AMP/ADC combinations indicates that the effects of integral nonlinearities are negligible; the slight difference in the statistical significance of the fits indicates that there are some residual differential nonlinearities (in ADC/AMP 1), but they are not large enough to negate our main conclusion: the hypothesis of a 17 keV neutrino

admixed with the electron neutrino with a mixing fraction of 0.8% is rejected at a confidence level of 99.6%. To be on the conservative side, we have adopted the rejection limit from ADC/AMP 2, which gives the lower confidence level.

The sensitivity of our results to various systematic effects was tested by conducting fits (with and without a 0.8% 17 keV neutrino) in which the following parameters have been modified: (1) The normalization of the subtracted background spectrum was changed by  $\pm 6\%$ . (2) The normalization of the subtracted  $^{137}\text{Cs}$  spectrum was changed by  $\pm 4\%$ . (3) The normalization of the subtracted pileup spectrum was changed by  $\pm 0.5\%$ . (4) The starting bin used in the compression was changed. Since the data were binned by summing every eight ADC channels together, we performed fits where the first channel used was 1, 2,  $\dots$ , 8. This should test for any periodicity in the differential nonlinearity in the ADC. (5) The energy calibration of the IB spectrum was changed by (a) shifting the zero by  $\pm 15$  eV, (b) changing the linear term by the error obtained from the energy calibration fit, and (c) using a quadratic energy calibration, instead of a linear one. (6) The flat tail term in the detector response function was changed by  $\pm 10\%$ . (7) Different efficiency curves were generated by (a) omitting the low energy points in the efficiency data, (b) using data obtained with the  $^{182}\text{Ta}$  source at 6 cm instead of those obtained at 8 cm, and (c) replacing the intensities of the  $^{182}\text{Ta}$  lines (from Ref. [26]) with those from Ref. [29]. The latter differ slightly from those of Ref. [26] at the lower energies. (8) A quadratic shape factor [ $P(E) = 1 + a_1(E - 151) + a_2(E - 151)^2$ ] was tried. The fits were conducted on the data set through ADC/AMP 2 (0.266 keV binning, 114 data points). The  $\chi^2$  for a fit with an admixture of a 0.8% 17 keV neutrino was always higher than the  $\chi^2$  for a single massless neutrino by 9 units or more. Because of the concern raised by Ref. [30] about the possibility that a large fraction of the difference between the  $\chi^2$  for a massive neutrino and that for a massless neutrino is due to systematic effects near the end point, we have also performed fits which exclude up to the last 10 keV (120–140 keV), and obtained, again, a  $\chi^2$  for a 0.8% 17 keV neutrino that is 9 units higher than that for a massless neutrino.

The relevant parameters for fits with and without a 0.8% 17 keV neutrino for each AMP/ADC are shown in Table I. The systematic errors on each of the parameters were taken to be one-half of the range of values obtained

TABLE I. Fitting results.

	ADC/AMP 1		ADC/AMP 2	
	$m = 0$	$m = 17$ keV $\sin^2 \theta = 0.8\%$	$m = 0$	$m = 17$ keV $\sin^2 \theta = 0.8\%$
Data points	98	98	114	114
$\chi^2$	102.8	114.6	110.6	120.5
$Q_{\text{EC}}$ (keV) <sup>a</sup>	185.763	185.730	185.771	$185.738 \pm 0.05 \pm 0.03$ <sup>b</sup>
$r$	1.04	1.06	1.03	$1.05 \pm 0.06 \pm 0.03$
$a_1$ (MeV <sup>-1</sup> )	-0.59	0.48	-0.63	$-0.03 \pm 0.12 \pm 0.9$

<sup>a</sup> $Q_{\text{EC}} = Q_0 + 35.492$  keV.

<sup>b</sup>Errors are  $\pm$  statistical  $\pm$  systematic and are the same for all entries in the same row.

in the systematics fits described above. The statistical errors are the one standard deviation errors obtained from the fits. Our EC  $Q$  value ( $Q_{\text{EC}} \equiv Q_0 + 35.492$ ) of  $185.77 \pm 0.05(\text{stat}) \pm 0.03(\text{syst})$  keV is within one standard deviation from the value  $186.1 \pm 0.3$  keV reported by Borge *et al.* Their value was obtained from fits to IB spectra using a nonrelativistic theory, however, and we believe the difference between the two results is essentially due to their use of the nonrelativistic theory. Indeed, we had also initially [31] performed fits using their theoretical model and obtained  $Q_{\text{EC}} = 186.94 \pm 0.06$  keV, which is in better agreement with their result. As we demonstrate shortly, the relativistic model of Surić *et al.* [21] is in better agreement with our data than the nonrelativistic model of Borge *et al.* [17], and therefore the  $Q_{\text{EC}}$  value we present here should be more accurate than both our preliminary value [31] and that of Borge *et al.* Our value is in disagreement with the value of  $179.3 \pm 2.0$  keV obtained by Flower *et al.* [22].

The shape parameter  $a_1 = -0.63 \pm 0.12 \pm 0.9$  MeV<sup>-1</sup> is small and corresponds to a change  $P(120 \text{ keV}) - P(150 \text{ keV})$  of 1.9% over the 30-keV fitting interval. With the effect of systematics taken into account it corresponds to a change that ranges from -0.9% to +4.5%. In comparison, Borge *et al.*, who used a shape factor of the form  $P(E) = \exp[\alpha(E - 110 \text{ keV})]$ , get  $\alpha = -3 \times 10^{-3}$  for one of their spectra and  $\alpha = -4.5 \times 10^{-3}$  for the other. These values of  $\alpha$  correspond to changes of +9.4% and +14.5%, respectively, over our 30-keV fitting interval. Hence our values are at least a factor of 2 smaller than those of Borge *et al.* We believe this difference is due primarily to our use of the relativistic IB calculations of Surić *et al.* Indeed, when we performed fits using Borge's nonrelativistic theoretical IB spectra we obtained shape factors which were much closer to theirs.

The scaling factor  $r = 1.03 \pm 0.06 \pm 0.03$  of the  $n = 3$  IB spectra is consistent with unity, and justifies, *a posteriori*, our setting of the normalization factors for  $n \geq 4$  IB spectra (whose contribution is small compared to that of the  $n = 3$  spectrum) to 1. Figure 8 shows the net IB spectrum together with the  $n = 2$  and  $n > 2$  components of the fit with a massless neutrino. The figure demonstrates the sensitivity of our data to the  $n \geq 3$  partial IB spectra.

Because of the closer agreement of the shape factor with unity, and the correct prediction of the ratio of the  $n \geq 3$  to  $n = 2$  partial IB spectra, we believe the relativistic calculation of Surić *et al.* is superior (in the sense that it gives better agreement with the data) to that of Borge's nonrelativistic calculation. The energy region which we fitted in our search for the 17 keV neutrino is dominated by  $p$  IB spectra, and, as mentioned earlier, no attempt was made to extract the relative contributions of the  $s$  and  $p$  IB components in these fits. Since Borge *et al.* obtained  $0.45 \pm 0.15$  for the scaling factor of  $s$  IB spectra (which indicates that their calculation does not give the correct relative intensities of  $s$ - to  $p$ -IB spectra), we were interested in seeing if this was the case for Surić's calculations too. Therefore we performed a fit over the energy region 110–150 keV (which includes the last 8 keV of the  $1s$  IB spectrum), in which

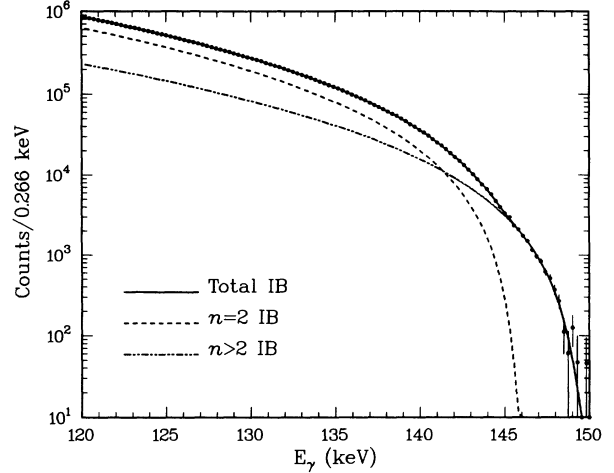


FIG. 8. Experimental IB spectrum, after pileup, background and contaminant subtraction. The solid line is the fit for  $m = 0$ ; the dashed line is the contribution of the  $n = 2$  IB spectra, the dash-two-dotted line is the contribution of the  $n > 2$  IB spectra.

the scaling factor  $r_{1s}$  of the  $1s$  IB spectrum was allowed to vary freely. We obtained  $r_{1s} = 0.94 \pm 0.03 \pm 0.07$  with  $m = 0$ , and  $1.00 \pm 0.03 \pm 0.07$  with  $m = 17$  keV,  $c = 0.8\%$ . The proximity of this factor to unity is another indication that Surić *et al.*'s calculation reproduces IB spectra very well, and justifies equating the scaling factors of the different  $j$  components (for  $n \geq 2$ ) in our fits.

## V. CONCLUSIONS

To summarize, we have searched for evidence of the admixture of a 17 keV neutrino with the electron-type neutrino in the IB spectrum accompanying the electron capture decay of <sup>125</sup>I. We reject the hypothesis of a 17 keV neutrino admixed with the electron neutrino with a mixing fraction of 0.8% at a confidence level  $\geq 99.6\%$ . Our upper limit for the admixture of a 17 keV neutrino is 0.4% at the 90% confidence level. We obtain an improved  $Q_{\text{EC}}$  value of  $185.77 \pm 0.06$  keV, which is in agreement with the value  $186.1 \pm 0.3$ , obtained by Borge *et al.* [17], but in disagreement with the most recent value of  $179.3 \pm 2.0$  keV, obtained by Flower *et al.* [22]. We also find that the recent calculations of Surić *et al.* [21] reproduce the shape and relative intensities of IB partial spectra within our systematic uncertainty of a few percent.

## ACKNOWLEDGMENTS

The assistance of James G. Parker in collecting the data is gratefully acknowledged. We would also like to thank Dr. T. Surić and Dr. I. Žliven for providing us with the code for calculating the IB matrix elements, and Dr. E. B. Norman for providing us with the <sup>182</sup>Ta source. This work was supported by the U.S. Department of Energy, Nuclear Physics Division, via Grant No. DE-FG05-87ER40314.

- [1] J. J. Simpson, Phys. Rev. Lett. **54**, 1891 (1985).
- [2] A. Hime and J. J. Simpson, Phys. Rev. D **39**, 1837 (1989).
- [3] B. Sur *et al.*, Phys. Rev. Lett. **66**, 2444 (1991).
- [4] J. J. Simpson and A. Hime, Phys. Rev. D **39**, 1825 (1989).
- [5] A. Hime and N. A. Jelley, Phys. Lett. B **257**, 441 (1991).
- [6] A. Hime, Oxford University, Report No. OUNP-91-20, 1991 (unpublished).
- [7] I. Žliven *et al.*, Phys. Rev. Lett. **67**, 560 (1991).
- [8] G. R. Kalbfleisch, P. Skierkowski, and M. Bahran, in *Neutrino Masses and Neutrino Astrophysics*, Proceedings of the Fourth Telemark Conference, Ashland, Wisconsin, 1987, edited by V. Barger, F. Halzen, M. Marshak, and K. Olive (World Scientific, Singapore, 1987), p. 366.
- [9] M. Bahran and G. R. Kalbfleisch, in *Proceedings of the Joint International Lepton-Photon Symposium and Europhysics Conference on High Energy Physics*, Geneva, Switzerland 1991, edited by S. Hegarty, K. Potter, and E. Quercigh (World Scientific, Singapore, 1992), p. 606.
- [10] T. Altzitzoglou *et al.*, Phys. Rev. Lett. **55**, 799 (1985); V. M. Datar *et al.*, Nature **318**, 547 (1985); T. Ohi *et al.*, Phys. Lett. **160B**, 322 (1985); J. Markey and F. Boehm, Phys. Rev. C **32**, 2215 (1985); A. Apalikov *et al.*, Pis'ma Zh. Eksp. Teor. Fiz. **42**, 233 (1985) [JETP Lett. **42**, 289 (1985)].
- [11] J. L. Mortara, I. Ahmad, K. P. Coulter, S. J. Freedman, B. K. Fujikawa, J. P. Greene, J. P. Schiffer, W. H. Trzaska, and A. R. Zeuli, Phys. Rev. Lett. **70**, 394 (1993).
- [12] G. E. Berman, M. L. Pitt, F. P. Calaprice, and M. M. Lowry, Phys. Rev. C **48**, R1 (1993).
- [13] D. W. Hetherington *et al.*, Phys. Rev. C **36**, 1504 (1987); D. Wark and F. Boehm, in *Nuclear Beta Decays and the Neutrino*, Proceedings of the International Symposium on Neutrino Mass and V+A Interactions, Osaka, Japan, 1986, edited by T. Kotani, H. Ejiri, and E. Takasugi (World Scientific, Singapore, 1986), p. 391.
- [14] H. Kawakami *et al.*, Phys. Lett. B **287**, 45 (1992).
- [15] F. E. Wietfeldt, Y. D. Chan, M. T. F. Da Cruz, A. Garcia, R.-M. Larimer, K. T. Lesko, E. B. Norman, R. G. Stokstad, and I. Žliven, Phys. Rev. Lett. **70**, 1759 (1993); I. Žliven *et al.*, Phys. Scr. **38**, 539 (1988).
- [16] D. E. DiGregorio, S. Gil, H. Huck, E. R. Batista, A. M. J. Ferrero, and A. O. Gattone, Phys. Rev. C **47**, 2916 (1993).
- [17] M. J. G. Borge, A. De Rújula, P. G. Hansen, B. Jonson, G. Nyman, H. L. Ravn, and K. Riisager, Phys. Scr. **34**, 591 (1986).
- [18] S. Schonert, K. Schreckenback, S. Neumaier, and F. von Feilitzsch, in *Electroweak Physics Beyond the Standard Model*, Valencia, Spain, 2-5 Oct. 1991 (World Scientific, Singapore, 1992), p. 155.
- [19] R. L. Kozub and M. M. Hindi, U.S. DOE Report No. DOE/ER/40314-6, 1992 (unpublished).
- [20] N. K. Sherman, Phys. Rev. Lett. **68**, 1434 (1992).
- [21] T. Surić, R. Horvat, and K. Pisk, Phys. Rev. C **47**, 47 (1993).
- [22] Sr. Flower, B. R. S. Babu, P. Venkataramaniah, and H. Sanjeeviah, Nuovo Cimento A **108**, 553 (1990).
- [23] S. Raman and N. B. Gove, Phys. Rev. C **7**, 1995 (1973).
- [24] W. Bambynek *et al.*, IAEA-TECDOC-619 (1991).
- [25] Yu. V. Sergeenkov and V. M. Sigalov, Nucl. Data Sheets **49**, 639 (1986).
- [26] T. Kempisty and K. Pochwalski, Nucl. Instrum. Methods Phys. Res. A **312**, 390 (1992).
- [27] F. B. Larkins, At. Data Nucl. Data Tables **20**, 313 (1977).
- [28] Note that we use the energy of the *first* channel of a binned data point for *both* the fitting function and the experimental data. That is, in our fits and in all the figures shown in the paper, the IB yield given at energy  $E$  is actually the total yield between  $E$  and  $E + \Delta E$ .
- [29] R. B. Firestone, Nucl. Data Sheets **54**, 307 (1988).
- [30] Moustafa Bahran and George R. Kalbfleisch, Phys. Rev. C **47**, R754 (1993).
- [31] R. L. Kozub and M. M. Hindi, U.S. DOE Report No. DOE/ER/40314-7, 1993 (unpublished).